

## Article

# High-Intensity Interval Training Induces Protein Lactylation in Different Tissues of Mice with Specificity and Time Dependence

Wenhua Huang <sup>1</sup>, Jie Su <sup>1</sup>, Xuefei Chen <sup>1</sup>, Yanjun Li <sup>1</sup>, Zheng Xing <sup>1</sup>, Lanlan Guo <sup>1,2</sup>, Shitian Li <sup>1</sup> and Jing Zhang <sup>1,\*</sup>

<sup>1</sup> School of P.E. and Sports Science, Beijing Normal University, Beijing 100875, China

<sup>2</sup> Department of Physical Education, University of International Business and Economics, Beijing 100029, China

\* Correspondence: zhangjing@bnu.edu.cn; Tel.: +86-010-58808038

**Abstract:** Protein lysine lactylation (Kla) is a novel protein acylation reported in recent years, which plays an important role in the development of several diseases with pathologically elevated lactate levels, such as tumors. The concentration of lactate as a donor is directly related to the Kla level. High-intensity interval training (HIIT) is a workout pattern that has positive effects in many metabolic diseases, but the mechanisms by which HIIT promotes health are not yet clear. Lactate is the main metabolite of HIIT, and it is unknown as to whether high lactate during HIIT can induce changes in Kla levels, as well as whether Kla levels differ in different tissues and how time-dependent Kla levels are. In this study, we observed the specificity and time-dependent effects of a single HIIT on the regulation of Kla in mouse tissues. In addition, we aimed to select tissues with high Kla specificity and obvious time dependence for lactylation quantitative omics and analyze the possible biological targets of HIIT-induced Kla regulation. A single HIIT induces Kla in tissues with high lactate uptake and metabolism, such as iWAT, BAT, soleus muscle and liver proteins, and Kla levels peak at 24 h after HIIT and return to steady state at 72 h. Kla proteins in iWAT may affect pathways related to glycolipid metabolism and are highly associated with de novo synthesis. It is speculated that the changes in energy expenditure, lipolytic effects and metabolic characteristics during the recovery period after HIIT may be related to the regulation of Kla in iWAT.

**Keywords:** high-intensity interval training; lysine lactylation; energy metabolism; proteomics



**Citation:** Huang, W.; Su, J.; Chen, X.; Li, Y.; Xing, Z.; Guo, L.; Li, S.; Zhang, J. High-Intensity Interval Training Induces Protein Lactylation in Different Tissues of Mice with Specificity and Time Dependence. *Metabolites* **2023**, *13*, 647. <https://doi.org/10.3390/metabo13050647>

Academic Editors: Tiemin Liu, Hongmei Yan, Qiongyue Zhang and Ting Yao

Received: 18 March 2023

Revised: 5 May 2023

Accepted: 8 May 2023

Published: 9 May 2023



**Copyright:** © 2023 by the authors. Licensee MDPI, Basel, Switzerland. This article is an open access article distributed under the terms and conditions of the Creative Commons Attribution (CC BY) license (<https://creativecommons.org/licenses/by/4.0/>).

## 1. Introduction

Protein lysine lactylation (Kla) is a novel protein acylation reported in *Nature* in 2019 [1] which refers to the state in which lactyl-coenzyme A is covalently bound to lysine residues of proteins catalyzed by lysine acyltransferases. The concentration of lactate as a donor precursor is directly related to the level of lactylation, and existing studies have shown that lactylation plays an important role in the development of several diseases with pathologically elevated lactate levels, such as tumors and sepsis. Lactate accumulation in the tumor microenvironment promotes immunosuppression by inducing histone lactylation in tumor-infiltrating myeloid cells, thus upregulating methyltransferase-like 3 [2]; additionally, lactate-induced histone lactylation in melanoma promotes YTH structural domain family protein 2 expression, thus driving tumorigenesis [3]. Moreover, lactate promotes lactylation of high-mobility group box-1 in macrophages in sepsis and affects their survival [4]. In addition, elevated lactate levels in the nervous system are also involved in neuroexcitation and anxiety-induced behavioral abnormalities in brain cells, as well as Alzheimer's disease-induced dysfunction, through protein lactylation [5,6]. Zhang et al. found that, in isolated cultured human HeLa cells and mouse bone marrow-derived macrophages, accumulated lactate following enhanced glycolysis by rotenone treatment similarly induced protein lactylation. These studies suggest that elevated lactate levels

in vivo may act biologically through a novel mechanism of protein lactylation [1]. However, the effect of elevated lactate levels that are induced during exercise on protein lactylation in the body has not been reported, and its biological role is currently unknown.

High-intensity interval training (HIIT) is a form of exercise in which short periods of high-intensity exercise and low-intensity exercise/rest are alternated and repeated several times [7]. Numerous studies have confirmed the positive effects of HIIT on fat loss, cardiovascular disease, diabetes, sarcopenia and nonalcoholic fatty liver disease [8–10]; however, the mechanism of action of HIIT for health promotion is not yet clear. Lactate is the main metabolite of HIIT, and it is currently unknown as to whether repeated and multiple exposures of the body to high lactate during HIIT can induce changes in lactylation levels, as well as whether lactylation levels differ in different tissues and how time-dependent lactylation levels are.

A large number of studies have shown that exercise modulates protein acylation as an important mechanism for health improvement, with some studies reporting that exercise is involved in the promotion of cognitive function in the nervous system by regulating histone acylation in the hippocampus [11]. In addition, exercise also influences exercise effects and metabolic health by modulating the acylations of various proteases in skeletal muscle [12]. The role of altered lactylation induced by high-intensity interval training in health is of interest [13].

In this study, we aimed to perform a whole-protein pan-Kla-level assay in HIIT mice and collect tissues of cardiac muscle, skeletal muscle, white fat, brown fat, liver and brain at multiple time points during rest and after exercise to observe the specificity and time-dependent effects of single HIIT on the regulation of protein lactylation in body tissues. In addition, we aimed to select tissues with high KLa specificity and obvious time-dependent effects for lactylation quantitative omics, analyze the possible biological targets of HIIT-induced KLa regulation and explore the KLa mechanism of HIIT for health promotion.

## 2. Materials and Methods

### 2.1. Experimental Animal Grouping

Eight-week-old male C57/BL6 mice weighing  $23.23 \pm 1.09$  g were purchased from Beijing Vital River Laboratory Animal Technology Co., Ltd. (Beijing, China), experimental animal production license No. SCXK (Beijing) 2016-0006. Mice were randomly divided into the control group (Con) and the HIIT exercise group (HIIT), which were further divided into 0/2/24/48/72 h postexercise groups according to the different time points of sacrifice at the end of HIIT exercise. The mice were housed in separate cages at a room temperature of  $22 \pm 5$  °C, humidity of  $50 \pm 10\%$ , alternating light and dark cycles of 12 h and free access to food and water. All of the feedings were provided by Huafukang Animal Experimental Feed Factory (Beijing, China).

### 2.2. Exercise Protocol

Mice were first subjected to adaptive running platform exercise, and maximum running speed was determined by increasing the treadmill speed by 1 m/min every 2 min until the mice were unable to keep up with the treadmill speed for more than 10 consecutive seconds under light stimulation with a wooden stick to determine the maximum running speed ( $S_{max}$ ) [14]. The following HIIT exercise protocol was designed according to the maximum running speed: 40%  $S_{max}$  warm-up for 5 min, followed by 85%  $S_{max}$  exercise for 1.5 min plus 45%  $S_{max}$  exercise for 2 min in one set, repeated for 9 sets and ending with 40%  $S_{max}$  relaxation for 3 min.

The mice were subjected to HIIT exercise according to the protocol, and the mice were sacrificed immediately and at 2, 24, 48 and 72 h after the end of exercise.

### 2.3. Blood Lactate Assay in Mice

At different time points after exercise, blood was collected from the tail vein of mice for blood lactate determination, and blood lactate concentrations were measured by using

blood lactate test strips (EKF, Lactate-scout, Leipzig, Germany) and a lactate tester (EKF, Lactate-scout, Leipzig, Germany).

#### 2.4. Detection of Energy Expenditure in Mice

Energy expenditure in mice was measured by using the OxyletPro metabolic assay system (Panlab, Barcelona, Spain). The following procedures were performed: the mice were placed in a respiratory metabolic cage for 24 h to acclimatize before HIIT exercise, followed by the HIIT running exercise; immediately after the exercise, the mice were placed back into the respiratory metabolic cage and continuously monitored for 24 h to measure the data of energy consumption, oxygen consumption, activity and food intake after which their total energy consumption was calculated.

#### 2.5. Protein Extraction and Western Blotting

The inguinal white adipose tissue (iWAT), epididymal white adipose tissue (eWAT), brown adipose tissue (BAT), liver, heart, brain, soleus and gastrocnemius muscle tissues were collected from C57/BL6 mice. Tissues were homogenized in lysis buffer, and total protein was quantified. Protein solutions were separated via electrophoresis by using 10–12% Bis-Tris gels and transferred to polyvinylidene difluoride (PVDF) membranes. The membranes were incubated with 5% skim milk for 2 h and then incubated overnight at 4 °C with primary antibody (anti-L-lactyl lysine rabbit mAb, 1:1000, PTM-1401, Jingjie PTM BioLab Co. Ltd., Hangzhou, China; GAPDH, 1:8000, CST5174, Cell Signaling Technology, Boston, USA;  $\beta$ -actin, 1:4000, E030110, Earthox, San Juan Island, WA, USA) diluted in TBST, after which they were finally incubated for 1 h with secondary antibody (goat anti-rabbit IgG, 1:8000, Earthox, San Juan Island, WA, USA) diluted with TBST. Membranes were then washed three times with PBS-T. Chemiluminescence reagent (WBKLS0100, Millipore, Burlington, NJ, USA) and a luminescence imaging analyzer (Amersham Imager 680, General Electric, Boston, MA, USA) were used for protein band detection. The relative protein expression was analyzed based on the gray value for GAPDH or  $\beta$ -actin.

#### 2.6. Four-Dimensional Label-Free Lactylation Quantitative Proteomics and Analysis

Four-dimensional label-free lactylation quantitative proteomics in mouse iWAT was performed by Jingjie PTM BioLab Co., Ltd. (Hangzhou, China).

##### 2.6.1. Protein Extraction and Trypsin Digestion

Samples were removed from  $-80$  °C and then fully ground to powder with liquid nitrogen. The samples in each group were added to 4 times the volume of extraction buffer (containing 10 mM DL-dithiothreitol, 1% protease inhibitor cocktail, 3  $\mu$ M TSA and 50 mM NAM) for ultrasonic lysis. An equal volume of Tris-balanced phenol was added, and the samples were centrifuged at  $5500\times g$  at 4 °C for 10 min. The supernatant was collected, and 5 times the volume of 0.1 M ammonium acetate/methanol was added for precipitation overnight. The precipitate was successively washed with methanol followed by acetone. Finally, 8 M urea was used for redissolution, and the protein concentration was determined by using a BCA kit.

The protein in each sample was enzymatically hydrolyzed in equal quantities, and the volume was adjusted to be consistent with the lysate. Subsequently, 20% TCA was slowly added, and the sample was vortexed and allowed to precipitate at 4 °C for 2 h. Centrifugation was performed at  $4500\times g$  for 5 min, and the precipitate was washed with precooled acetone 2–3 times. After drying off the precipitate, 200 mM TEAB was added. Afterwards, trypsin was added at a ratio of 1:50 (protease: protein, M/M), and the sample was digested overnight. Dithiothreitol (DTT) was added to a final concentration of 5 mM, and the sample was reduced at 56 °C for 30 min. Iodine acetamide (IAA) was subsequently added to a final concentration of 11 mM, and the mixture was incubated for 15 min at room temperature in the absence of light.

### 2.6.2. Pan-Kla Antibody-Based PTM Enrichment

Peptides were dissolved in IP buffer solution (100 mM NaCl, 1 mM EDTA, 50 mM Tris-HCl, 0.5% NP-40, pH 8.0), and the supernatant was transferred to prewashed lactylation resin (antibody resin Art. 5798717296493442124, Hangzhou Jingjie Biotechnology Co., Ltd., PTM Bio, Hangzhou, China), placed on a rotating shaker at 4 °C and gently shaken overnight. After incubation, the resin was washed 4 times with IP buffer solution and twice with deionized water. Finally, 0.1% trifluoroacetic acid was used to elute the resin-bound peptide three times. The eluent was collected and vacuum dried. After being drained, the salt was removed according to the C18 ZipTips instructions (ZTC18S, Millipore, Burlington, NJ, USA); after being vacuum frozen and drained, the liquid was obtained for mass analysis.

### 2.6.3. Quantitative Proteomic Analysis via LC–MS/MS

The peptides were dissolved in buffer A and separated via ultra-performance liquid chromatography by using a nanoElute system. Buffer A was 0.1% formic acid and 2% acetonitrile in water. Buffer B was 0.1% formic acid in acetonitrile solution. The liquid phase gradient settings were as follows: 0–44 min, 6–22% B; 44–56 min, 22–30% B; 56–58 min, 30–80% B; 58–60 min, 80% B. The flow rate was maintained at 300 nL/min. Moreover, the peptides were separated, injected into the capillary ion source and analyzed by using a timsTOF Pro mass spectrometer.

### 2.6.4. Bioinformatics Analysis

Gene Ontology (GO) annotation of the proteome was performed with eggNOG-mapper software (version 2.0). Identified protein domain functional descriptions were annotated by using InterProScan (version 5.14-53.0) based on the protein sequence alignment method, and the InterPro domain database was used. The Kyoto Encyclopedia of Genes and Genomes (KEGG) database was used to annotate the protein pathways. These pathways were classified into hierarchical categories according to the KEGG website. All of the differentially expressed protein database accessions or sequences were searched against the STRING database (version 11.0) for protein–protein interactions. WoLF PSORT (version 0.2), which is subcellular localization prediction software, was used to predict subcellular localization. Soft MoMo (version 5.0.2) was used to analyze the model of sequences comprising amino acids in specific positions of modify-21-mers in all of the protein sequences.

## 2.7. Data Analyses and Statistics

In this study, data are presented as the mean  $\pm$  SD. Statistical analyses were performed by using one-way ANOVA followed by the Newman–Keuls posttest. A  $p$  value  $< 0.05$  was considered to be statistically significant. Prism (Version 9.0) was used to verify the normality of the data. Moreover, the cross-sectional area of adipocytes was calculated via ImageJ (Version 1.53a.). The grayscale values of the protein bands were calculated by using Image Processing and Analysis in Java (ImageJ, version 1.53a).

## 3. Results

### 3.1. Changes in Blood Lactate and Energy Expenditure after HIIT

The detailed exercise protocol and time points of sampling are shown in Figure 1A. Blood lactate concentrations after HIIT demonstrated a significant increase in blood lactate concentrations immediately after exercise ( $p < 0.01$ ); blood lactate concentrations then slowly decreased and remained higher than in the Con group 5 min after HIIT ( $p < 0.05$ ). Furthermore, blood lactate concentrations were not significantly different from the Con group after 15, 30 and 60 min (Figure 1B).

Changes in energy metabolism after HIIT showed that the energy expenditure of the HIIT group was higher than that of the Con group 24 h after HIIT exercise in mice, which occurred both during the daytime and nighttime (Figure 1C); in addition, the total energy expenditure of the HIIT group was significantly higher than that of the Con group

immediately after exercise, as well as at 2 h after exercise and 24 h after exercise ( $p < 0.01$ , Figure 1D).

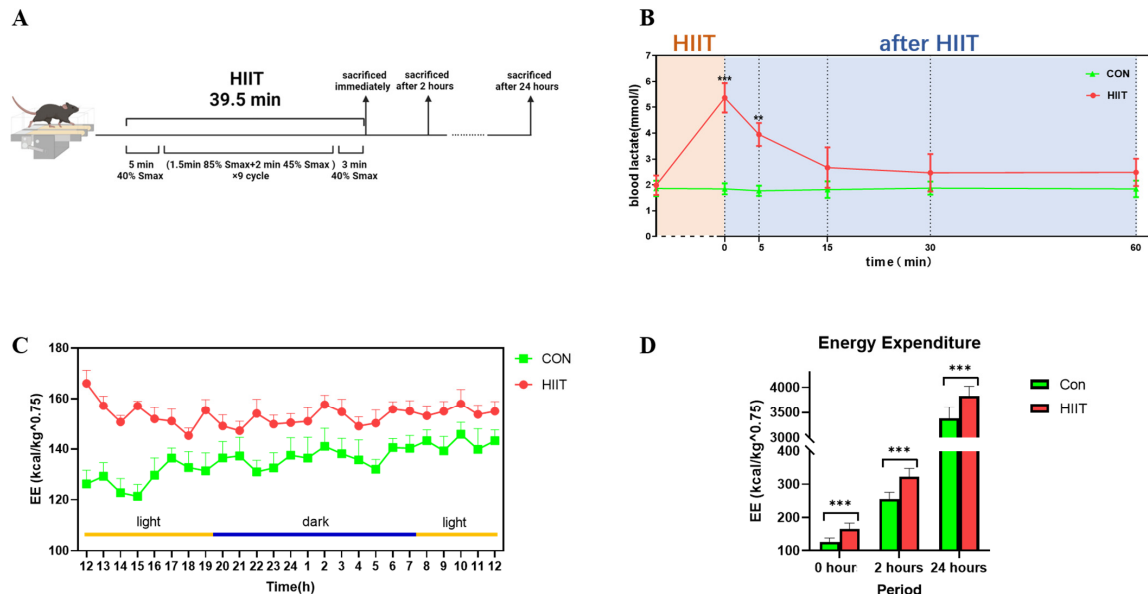


**Figure 1.** Changes in blood lactate and energy expenditure in mice after HIIT. (A) HIIT mouse protocol and sacrifice time; (B) blood lactate changes in Con and HIIT mice; (C) energy expenditure changes in Con and HIIT mice; and (D) energy expenditure in Con and HIIT mice at 0, 2 h and 24 h. \*\*  $p < 0.01$ , \*\*\*  $p < 0.001$ .

### 3.2. Effect of HIIT on Lactylation of Proteins from Different Tissues

#### 3.2.1. Effect of HIIT on Lactylation of Adipose Tissue Proteins

The Western blotting results showed that K1a levels were significantly higher in the 24 h group than in the Con group in iWAT ( $p < 0.05$ , Figure 2A); in BAT, K1a levels were significantly higher in the 0 h, 2 h and 24 h groups than in the Con group (0 h and 2 h:  $p < 0.05$ ; 24 h:  $p < 0.01$ , Figure 2B). Moreover, in eWAT, the time points were not significantly different (Figure 2C). This suggests that, in adipose tissue, K1a levels in iWAT and BAT appear to be idiosyncratically upregulated after HIIT.

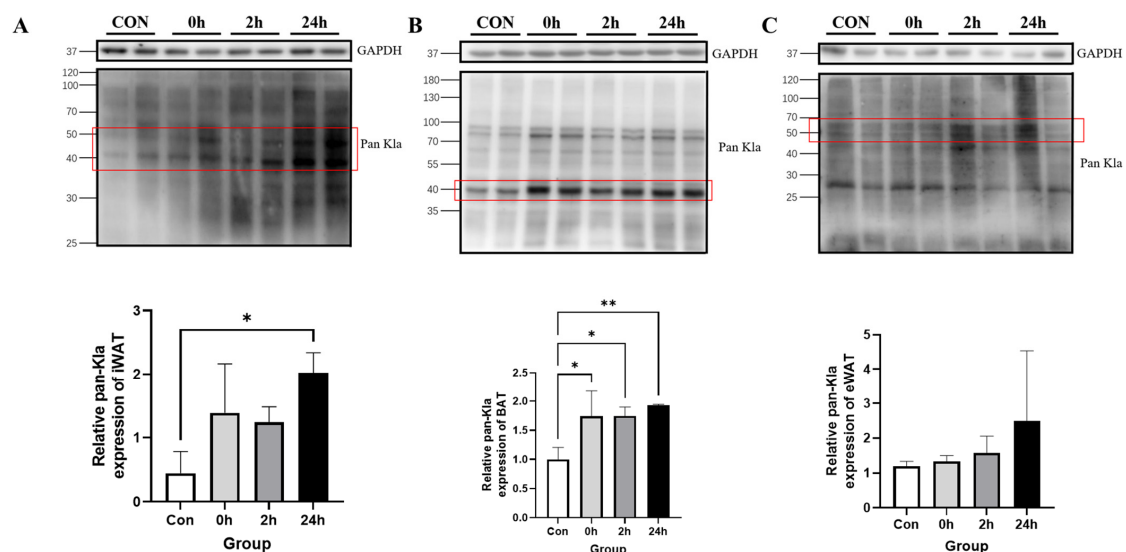


**Figure 2.** Changes in protein pan K1a in adipose tissue immediately, 2 h and 24 h after HIIT. (A) iWAT pan-K1a detection and quantification; (B) BAT pan-K1a detection and quantification; and (C) eWAT pan-K1a detection and quantification. \*  $p < 0.05$ , \*\*  $p < 0.01$ , the red squares are representative bands for statistical analysis.

### 3.2.2. Effect of HIIT on Lactylation of Cardiac and Skeletal Muscle Proteins

Western blotting results showed that K<sub>la</sub> levels were significantly higher in the 24 h group than in the Con group and at 0 h in the soleus muscle ( $p < 0.01$ , Figure 3A); additionally, there were no significant changes in K<sub>la</sub> levels at any time point in the cardiac and gastrocnemius muscles (Figure 3B,C). This indicates that there was a specific upregulation of K<sub>la</sub> levels after HIIT in the soleus muscle.

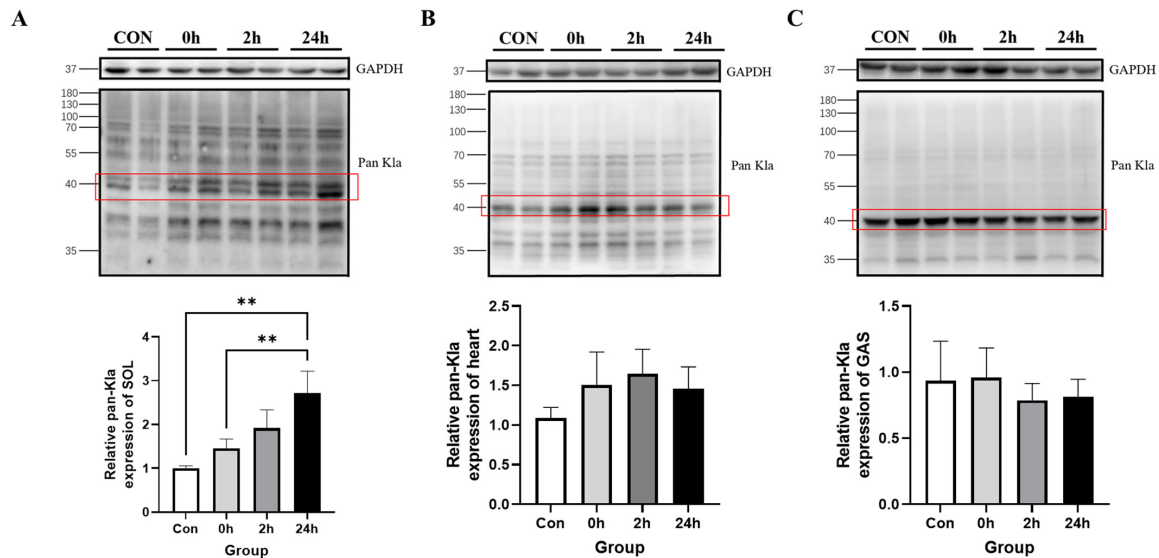


**Figure 3.** Changes in protein pan-K<sub>la</sub> in cardiac and skeletal muscle immediately, 2 h and 24 h after HIIT. (A) Soleus muscle pan-K<sub>la</sub> detection and its quantification; (B) heart pan-K<sub>la</sub> detection and its quantification; and (C) gastrocnemius muscle pan-K<sub>la</sub> detection and its quantification. \*\*  $p < 0.01$ , the red squares are representative bands for statistical analysis.

### 3.2.3. Effect of HIIT on Lactylation of Other Tissue Proteins

Western blotting results showed that K<sub>la</sub> levels were higher in the 24 h group than in the Con group in the liver ( $p < 0.05$ , Figure 4A); moreover, there was no significant change in K<sub>la</sub> levels at any time point in the brain (Figure 4B). This indicates that there was a specific upregulation of K<sub>la</sub> levels in the liver after HIIT.

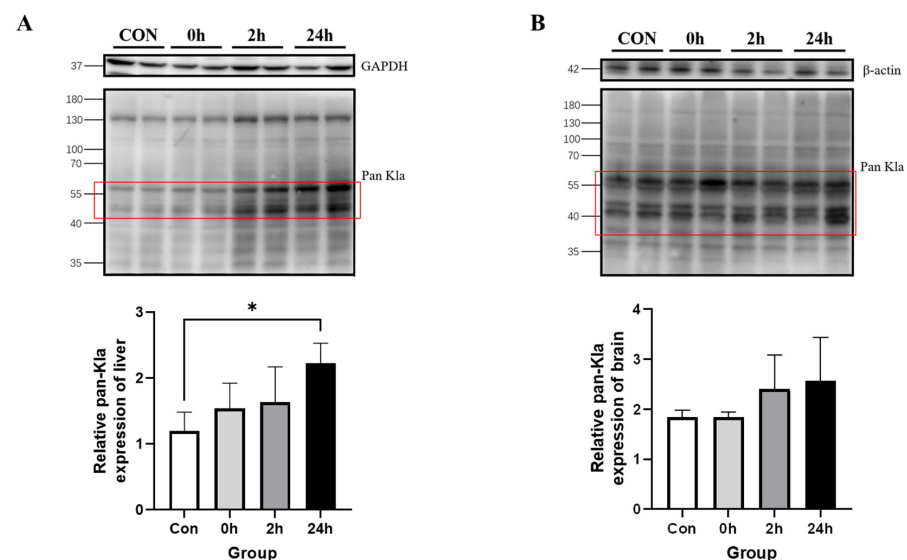


**Figure 4.** Changes in protein pan-K<sub>la</sub> in other tissues immediately, 2 h and 24 h after HIIT. (A) Liver pan-K<sub>la</sub> detection and quantification; (B) brain pan-K<sub>la</sub> detection and quantification. \*  $p < 0.05$ , the red squares are representative bands for statistical analysis.

### 3.2.4. Time-Dependent Effect of HIIT on Tissues with Specific Changes in Lactylation

The Western blotting results showed that iWAT, BAT, soleus muscle and liver had significantly increased K<sub>la</sub> levels within 24 h after HIIT. To explore the peaks and trends in K<sub>la</sub> levels after HIIT, these tissues were tested for changes in K<sub>la</sub> levels at 48 and 72 h after HIIT. The results showed that iWAT had significantly lower K<sub>la</sub> levels at 48 and 72 h than at 24 h ( $p < 0.05$ , Figure 5A); additionally, BAT had significantly lower K<sub>la</sub> levels at 72 h than at 24 h ( $p < 0.01$ , Figure 5B). Soleus muscle K<sub>la</sub> levels at 48 and 72 h remained significantly higher than that in the Con group ( $p < 0.05$ , Figure 5C); moreover, liver K<sub>la</sub> levels at 72 h were significantly lower than those at 24 h ( $p < 0.05$ , Figure 5D). It was demonstrated that K<sub>la</sub> levels in these tissues after HIIT peaked at 24 h and then declined in a stepwise fashion, with the vast majority of levels returning to steady state levels at 72 h.

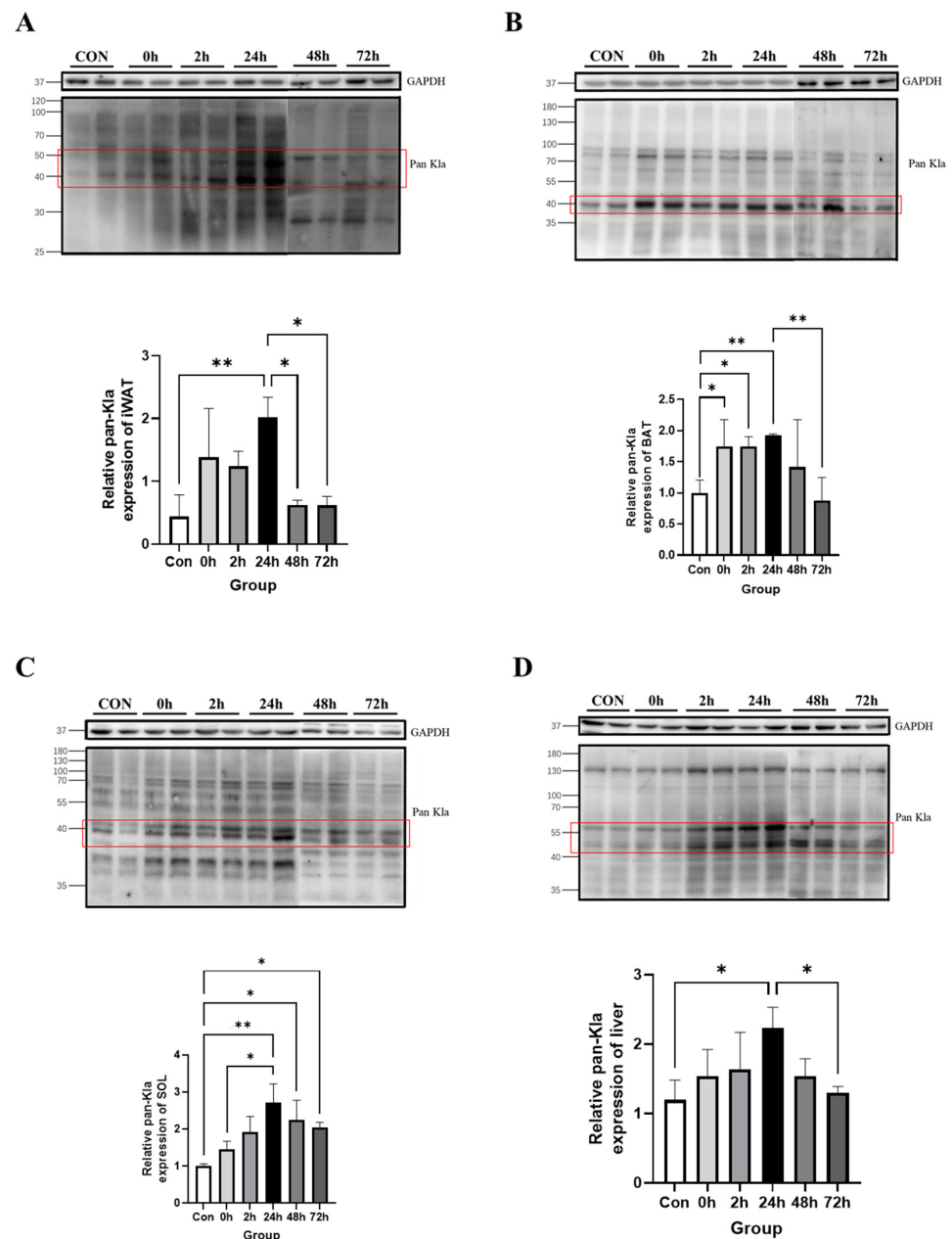


**Figure 5.** Changes in protein pan-K<sub>la</sub> in iWAT, BAT, soleus muscle and liver tissues after HIIT. (A) iWAT pan-K<sub>la</sub> detection and quantification; (B) BAT pan-K<sub>la</sub> detection and quantification; (C) soleus muscle pan-K<sub>la</sub> detection and quantification; and (D) liver pan-K<sub>la</sub> detection and quantification. \*  $p < 0.05$ , \*\*  $p < 0.01$ , the red squares are representative bands for statistical analysis.

### 3.3. Quantitative Proteomic Analysis of Lysine Lactylation in Mouse iWAT

#### 3.3.1. Kla-Upregulated Protein Screening

The iWAT lysine lactylation of quantitative proteomic results showed that there were 25 proteins and 37 sites of Kla modification that were upregulated in the HIIT group compared with the Con group (Figure 6A); detailed Kla upregulation site volcanoes and heatmaps of upregulated proteins are shown in Figure 6B,C. Among them, fatty acid synthetase (Fasn) had eight Kla upregulation sites, ATP-citrate lyase (Acly) had four upregulated sites, superoxide dismutase 1 (SOD1) and pyruvate carboxylase (PC) had two upregulated sites and all others had one upregulated site (Figure 6D).

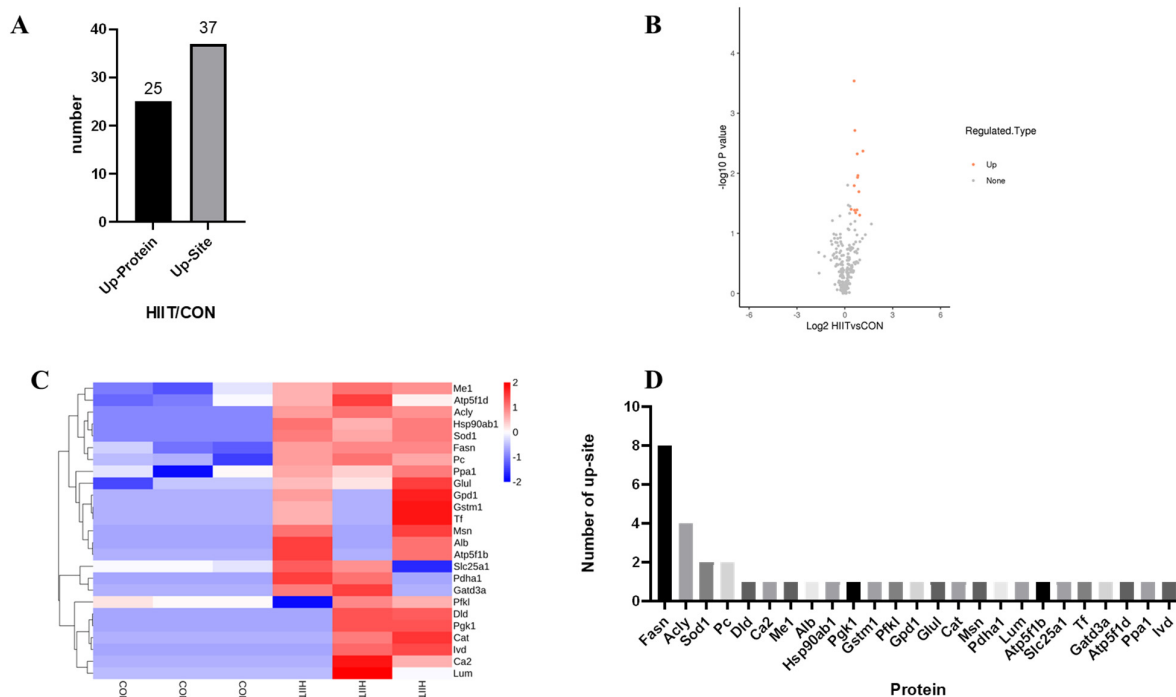


**Figure 6.** Screening of differentially Kla-upregulated proteins. (A) The number of iWAT Kla-upregulated proteins and sites; (B) volcano map of iWAT Kla-upregulated modification sites; (C) heatmap of iWAT Kla-upregulated proteins; and (D) the number of Kla sites for each iWAT-upregulated protein.

#### 3.3.2. Functional Classification of Kla-Upregulated Proteins

After classifying Kla-upregulated proteins according to GO and subcellular localization, the results of biological processes in GO showed that the vast majority of Kla-upregulated proteins are involved in metabolic and cellular processes; additionally, cellular components demonstrated that they are involved in cellular and extracellular compositions, and the molecular functions showed that they are overwhelmingly involved in adhesive and catalytic activities (Figure 7A). The subcellular localization classification showed that the vast majority of Kla-upregulated proteins were located in the cytoplasm (56%), followed by mitochondria (28%), extracellular space (12%) and nucleus (4%, Figure 7B). It is suggested that the screened differentially upregulated Kla proteins in iWAT (likely located in the cytoplasm and mitochondria) are involved in cellular metabolic processes, which are possibly regulated by molecular functions of complexes and catalytic activity.

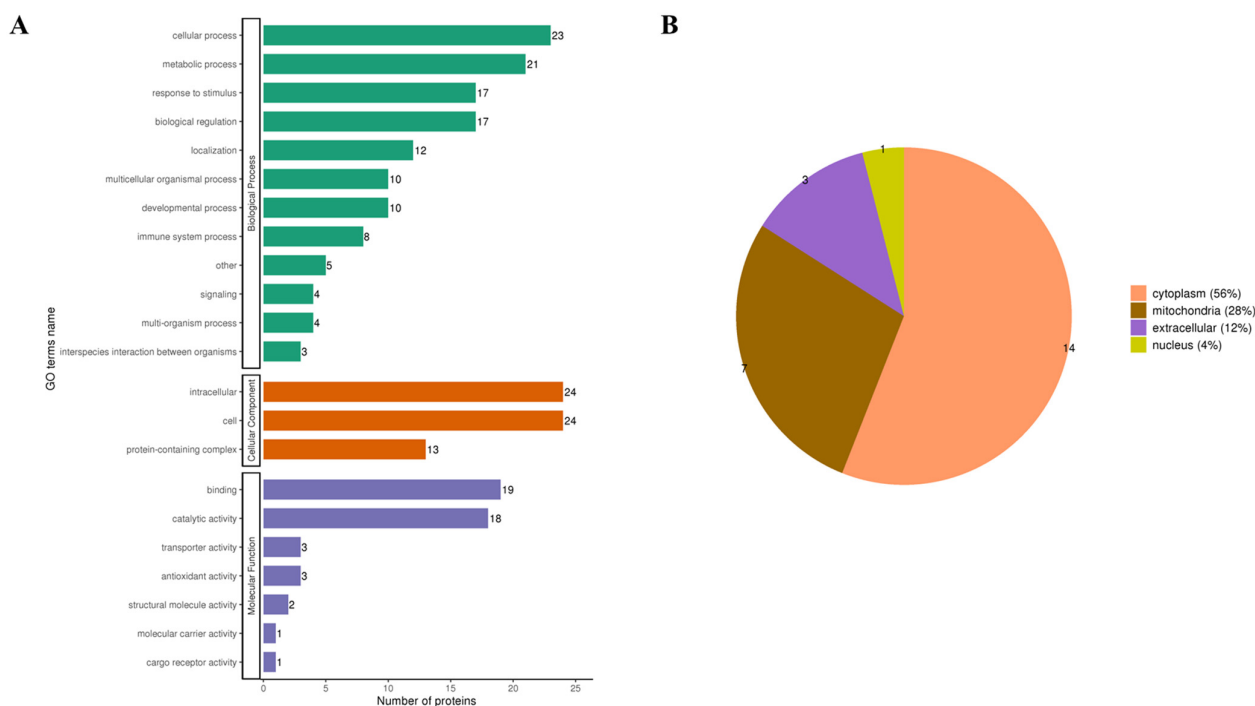


**Figure 7.** GO and subcellular localization classification of differentially Kla-upregulated proteins. (A) iWAT Kla-upregulated protein GO annotation classification; (B) iWAT Kla-upregulated protein subcellular structure annotation classification.

### 3.3.3. Kla Upregulates Protein GO Enrichment Function

For the annotation of all of the identified proteins and the screening of differentially upregulated proteins, we performed GO classification enrichment analysis comparing differentially upregulated proteins in the HIIT and Con groups to determine whether there was a significant trend of enrichment in certain functional types. The  $p$  values obtained from the enrichment test (Fisher's exact test) are presented as a bubble plot showing the functional categories and pathways in which differentially expressed proteins are significantly enriched ( $p < 0.05$ ). The results of the top 20 most significantly enriched categories are presented in bubble plots. Additionally, the vertical axis of the bubble plot is the functional classification or pathway, and the horizontal axis value is the  $\log_2$ -transformed value of the fold change in the proportion of differential proteins in that functional type compared to the proportion of identified proteins. Moreover, the circle color indicates the enrichment significance  $p$  value, and the circle size indicates the number of differential proteins in the functional classification or pathway.

Enrichment analysis of molecular functions showed that proteins involved in hydrolyase, ATP, NADP and phosphatase binding were lactylated at higher levels after HIIT (Figure 8A); additionally, enrichment analysis of cellular components showed that proteins involved in secretory vesicles, myelin and pyruvate dehydrogenase complexes were lactylated at higher levels (Figure 8B). Furthermore, enrichment analysis of biological processes showed that proteins were involved in phospho-nucleoside metabolic processes, organic phosphate biosynthesis, coenzyme biosynthesis and dicarboxylic acid metabolism (Figure 8C). From the GO perspective, it is suggested that HIIT-induced lactylation of iWAT proteins may mediate changes in the biological processes of energy metabolism through various enzymes and binding processes related to glycolipid metabolism.

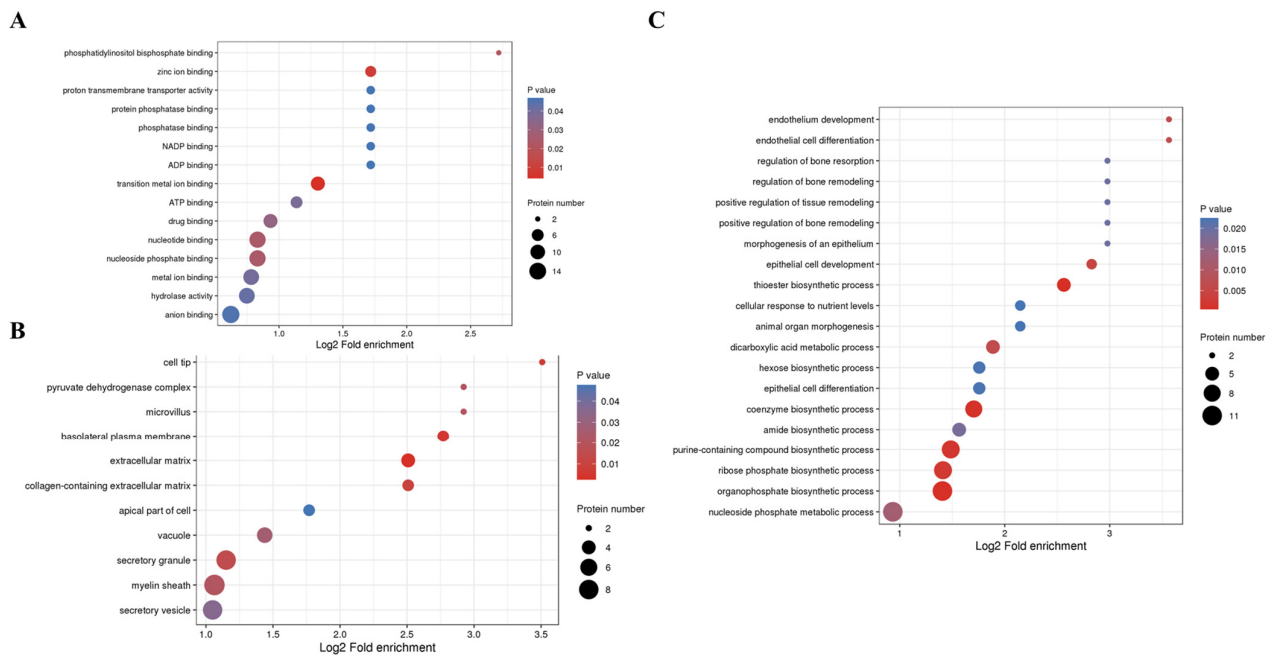


**Figure 8.** Functional analysis of GO enrichment of iWAT differentially Kla-upregulated protein. (A) Molecular function of iWAT Kla-upregulated protein enrichment; (B) cellular component of iWAT Kla-upregulated protein enrichment; and (C) biological processes of iWAT Kla-upregulated protein enrichment.

### 3.3.4. KEGG Enrichment Pathway of Kla-Upregulated Proteins

KEGG is an information network linking known molecular interactions, and the differentially Kla-upregulated protein KEGG pathway that was obtained from the above-mentioned enrichment analysis was visualized in the form of a web page, with the differentially upregulated protein indicated in red in the figure. The results showed that differentially Kla-upregulated proteins were mainly enriched in the tricarboxylic acid cycle, pyruvate metabolism, glycolysis/gluconeogenesis and oxidative phosphorylation metabolic pathways (Figure 9). Moreover, KEGG further supported the abovementioned speculation of GO enrichment, and all four enriched pathways were highly related to glycolipid metabolism and energy metabolism, thus suggesting that HIIT-mediated iWAT lactylation proteins may be involved in the regulation of energy metabolism.

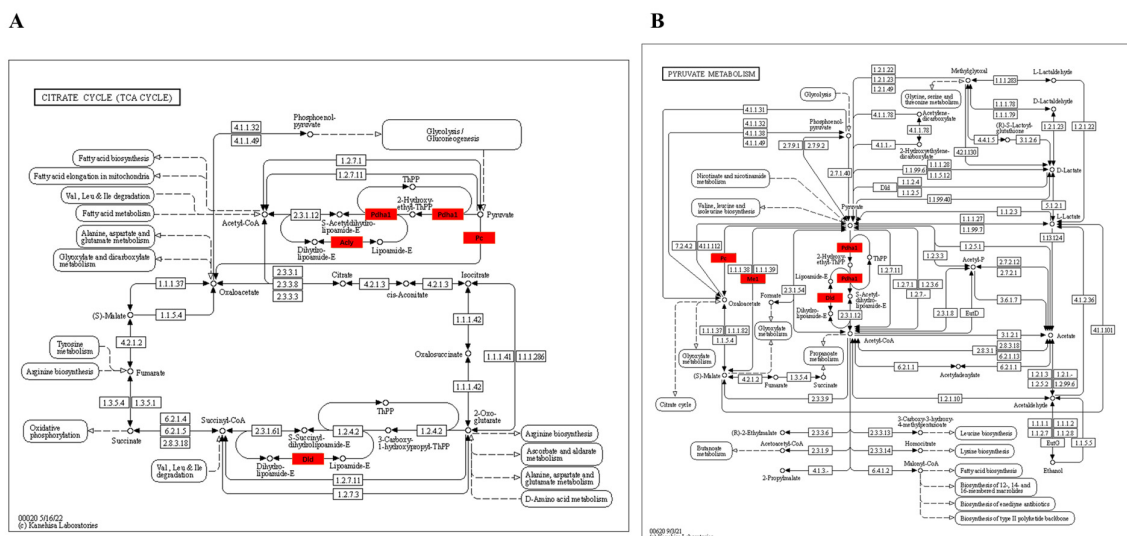


**Figure 9.** Cont.

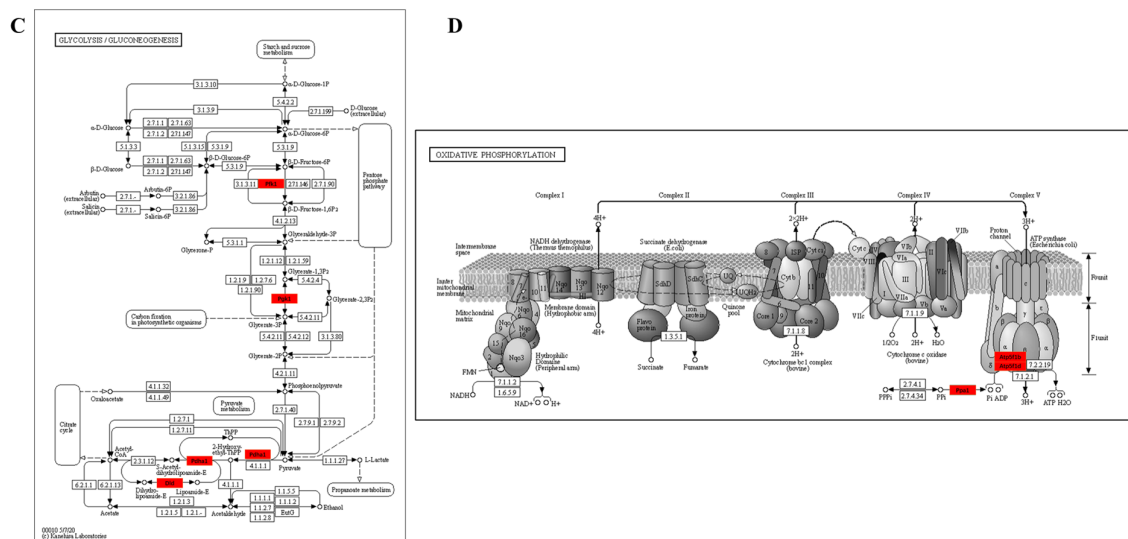


**Figure 9.** Functional analysis of GO enrichment of iWAT differentially Kla-upregulated protein. (A) iWAT Kla-upregulated protein enriched citrate cycle pathway; (B) iWAT Kla-upregulated protein enriched pyruvate metabolic pathway; (C) iWAT Kla-upregulated protein enriched glycolysis/gluconeogenesis pathway; and (D) iWAT Kla-upregulated protein enriched oxidative phosphorylation pathway. The names of the proteins in the red squares are Kla up-regulated proteins. The original KEGG pathway diagram can be viewed at [www.kegg.jp](http://www.kegg.jp).

## 4. Discussion

Lactate is the most well-known small molecule in the field of sports science; from early time periods, it was referred to as a “metabolic waste”, and in later time periods, it was known as an “energy fuel”. Lactate is also classified as being a metabolic small molecule and signaling molecule. The role of lactate in exercise is again becoming a focus of research [15].

### 4.1. Tissue Specificity of HIIT-Induced Kla

The mice were sacrificed and sampled immediately and 2 h and 24 h after HIIT, and different tissues were examined for protein pan-Kla. To facilitate the quantification of Kla levels, representative bands with significant Kla levels in each tissue were selected for quantitative analysis.

The effects of exercise on protein lactylation in different tissues have not yet been reported. In this study, HIIT was found to induce upregulation of protein lactylation levels in iWAT, BAT, soleus muscle and liver and they peaked at 24 h.

The results of this study suggest that the lactylation that occurs postexercise is tissue-specific, and lactylation mainly occurs in metabolically active tissues such as the soleus muscle, adipose tissue and liver, which also have the characteristics of lactate metabolism and are sites of lactate uptake, removal and utilization. Representative tissues for lactate for oxidative energy supply are the soleus muscle and cardiac muscle; specifically, slow-twitch fibers have a large amount of monocarboxylate transporter 1 (MCT1) that is responsible for transporting lactate into myocytes, as well as little MCT4 responsible for the outward transport of lactate [16]. During exercise, MCT1 mediates the entry of lactate into slow-twitch fibers for direct oxidative energy supply. The healthy liver has a higher net lactate clearance than any other organ, accounting for 70% of systemic clearance [17]. Moreover, lactate uptake by adipose tissue during exercise may be a way to address elevated blood lactate levels and may promote adipose tissue browning [18,19]. In addition to its otherwise known functions in these metabolically active tissues, the present study found that lactate may play other biological roles by promoting protein lactylation.

Numerous previous studies have reported that exercise induces muscle and liver acylation levels and is associated with changes in metabolite levels [20–24]. Our study likewise implies that lactate produced by exercise may induce similar effects.

In the brain, gastrocnemius and eWAT K<sub>la</sub> levels did not significantly change after exercise, which is likely due to the fact that these tissues are not the main locations where blood lactate is taken up for metabolism. The presence of the blood-brain barrier makes it difficult for blood lactate to enter the brain; moreover, the very small amount of blood lactate that enters the brain during exercise is also directly oxidized for energy supply [25]. The gastrocnemius muscle is anaerobically glycolytically energized in HIIT, thus producing large amounts of lactate that are transported out of the myocyte via MCT4 and that enters the circulation through the lactate shuttle; additionally, the gastrocnemius muscle has reduced lactate levels and is the most important producer (rather than utilizer) of lactate during exercise [26]. The abovementioned study suggests that the lactate level of the tissue may be responsible for influencing its lactylation level.

In addition to lactate concentration as an influence of K<sub>la</sub> donors, both lactyltransferase and deacetylases (HDACs) are important influencing factors; however, there are fewer studies on exercise intervention of acylated metabolizing enzymes, and the relationship between these factors is uncertain. It has been found that lactate also inhibits the activity of protein HDACs [27,28], which are the specific deacylases in K<sub>la</sub> [29]. This scenario may also be one of the reasons why lactate produced by HIIT idiosyncratically regulates the increased levels of K<sub>la</sub>.

#### 4.2. Time Dependence of HIIT-Induced K<sub>la</sub>

Exercise induces a differential regulation of the time-dependent nature of different posttranslational modifications (PTMs). A time-dependent effect of exercise on PTMs of skeletal muscle in animals and humans has been reported in previous studies [30,31]. It is evident that PTMs are dynamic modifications that take time to change [32]. However, there are no straightforward studies on the time dependence of changes in the level of lactylation after exercise.

In this study, changes in K<sub>la</sub> levels were continuously observed for 72 h after a single HIIT exercise session, and several tissues were found to have a stepwise increase in K<sub>la</sub>, wherein it peaked at 24 h and then gradually reduced. This is similar to the results of previous K<sub>la</sub> kinetic (24 h) studies; specifically, the activation of bone marrow-derived macrophages (BMDMs) with lipopolysaccharide and interferon- $\gamma$  resulted in a significant increase in K<sub>la</sub> after 16 h, peaking at 24 h [1]. In addition, after the treatment of BMDMs with lactate BMDMs, K<sub>la</sub> significantly increased after 24 h [33]. Most of the current studies have examined changes during the 24 h following the induction of K<sub>la</sub>; changes in K<sub>la</sub> levels after 24 h have not been reported. Our results showed that iWAT, BAT and liver K<sub>la</sub> levels quickly decreased, whereas K<sub>la</sub> levels in soleus muscle slowly decreased. However, the regulatory mechanism responsible for this effect is unclear.

In this study, we observed that HIIT, in addition to producing large amounts of lactate, increased excess postexercise oxygen consumption and postexercise energy metabolism. After HIIT, the energy expenditure of mice was higher than that of control mice for 24 h, and the total energy metabolism was significantly higher than that of control mice immediately and 2 h and 24 h after HIIT. These results are in good agreement with the time-dependent regulation of tissue protein lactylation. Although the effect of elevated blood lactate by HIIT rapidly disappeared, the effect of enhanced energy metabolism was maintained for more than 24 h. It is hypothesized that HIIT-induced enhancement of lactylation is involved in promoting energy expenditure by regulating the biological functions of multiple proteins.

#### 4.3. Biological Effects of HIIT-Induced K<sub>la</sub>

One of the characteristics of HIIT in training scenarios is its powerful fat loss effect and postexercise energy depletion effect. In this study, we found that the K<sub>la</sub> level of iWAT showed significant changes after HIIT, which increased with time. iWAT is the main tissue

affected by HIIT and is closely related to the purpose and effects of exercise. Moreover, iWAT K<sub>la</sub> level changes are related to metabolic remodeling, which is a new entry point to elucidate the effect of HIIT; thus, 4D label-free lactylation quantitative omics was used to detect differential proteins and sites of lactylation in iWAT.

As a type of acylation, K<sub>la</sub> has many characteristics in common with other acylations. The first commonality is that it occurs on histone and nonhistone proteins and has different effects on function. The vast majority of current reports on lactylation concern histone lactylation and fewer are on nonhistone lactylation. When histones are modified by acylation, they promote gene transcription and expression, whereas nonhistone acylations cause changes in protein structure, which correspondingly alter protein interactions. Furthermore, acylations that occur in metabolic regulatory proteins tend to inhibit enzyme activity and impair metabolic processes.

The classification of subcellular localization by lactylation quantitative proteomics demonstrated that more than 80% of the lactylation proteins in iWAT are localized in the cytoplasm and mitochondria, which are the most active locations for cellular substance metabolism and energy metabolism; in addition, the nonhistone K<sub>la</sub> may affect their active functions.

The same GO classification of biological processes demonstrated a high percentage of lactylation proteins involved in phosphonucleoside metabolic processes and organophosphate biosynthesis processes, which are important components of energy metabolism and life processes [34]. Additionally, coenzyme biosynthesis processes and dicarboxylic acid metabolism processes have a higher degree of K<sub>la</sub>, which are equally related to metabolic homeostasis, glucose metabolism and amino acid metabolic processes [35–37]. The above-mentioned GO analysis demonstrated HIIT-induced lactylation of iWAT protein, which seems to be closely related to the process of material energy metabolism.

KEGG-enriched pathways were demonstrated to be mainly enriched in the tricarboxylic acid cycle, pyruvate metabolism, glycolysis/glycogenesis and oxidative phosphorylation metabolic pathways. Several reports have suggested a close relationship between these pathways in fat loss, fat browning and metabolic regulation [38–41]. The enrichment pathways of K<sub>la</sub>-upregulated proteins in KEGG are all highly correlated with glucolipid metabolism and energy, which may be one of the reasons why HIIT regulates lipid metabolism.

In our experiments, we verified that energy expenditure after HIIT was significantly higher in mice than in control mice and that energy expenditure after HIIT mainly originated from lipid metabolism [42]. Additionally, in this study, we found that both iWAT and BAT proteins exhibited increased K<sub>la</sub> levels; thus, it is speculated that the K<sub>la</sub> of proteins in adipose tissue may be related to their metabolic activity.

The lactylation quantitative proteomics results revealed that lactate produced by HIIT induced K<sub>la</sub> of several proteins and sites in iWAT, most notably Fasn and Acly, with eight and four sites of lactylation being observed, respectively. In contrast, Fasn and Acly are the key proteases for de novo lipogenesis [43], and they are the core proteins that control fat metabolism [44]. The acetylation of Fasn and Acly has been found to affect their stability and activity, thus affecting their functions [45,46]. Although K<sub>la</sub> is acylated and acetylated [47], it is possible that these proteins produce the same effects after K<sub>la</sub> is acylated, which can possibly affect the metabolic process of de novo lipogenesis and mediate a greater rate of HIIT lipolysis than MICT lipolysis. In addition, it has been found that Fasn can be lactylated and affect lipid metabolism in nonalcoholic fatty liver disease [48].

Based on the abovementioned evidence, it can be speculated that the lipid metabolic effects resulting after HIIT may be related to the action of lactate, and one of the mechanisms of this regulation of lipid metabolism may be closely related to the modifications of lipid metabolism-related enzymes.

The present study still has some limitations: (1) the effect of long-term HIIT on lactylation in each tissue could not be investigated in our study, and whether the long-term

effect is consistent with single HIIT deserves further confirmation. (2) In addition, this study used only Western blotting as a screen for tissue-specific changes in lactylation after HIIT, which may not be completely accurate. The regulation of lactylation is diverse, both elevated and decreased, and measuring the precise effect of HIIT on lactylation of tissues also requires histology to be combined with lactylation proteomics.

This report investigates which tissues HIIT may affect regarding the specific upregulation of lactylation, providing a direction and basis for further subsequent targeting of lactylation-mediated biological functions and functional validation of target proteins in different tissues; the specificity of the upregulation of tissue lactylation levels after HIIT was also explored, mainly from the perspective of lactate metabolism, and the existence of specific regulation of related metabolic enzymes also deserves further attention; the exact mechanisms accounting for the time-dependent changes in tissue lactylation after HIIT are not yet clear and equally deserve further exploration.

## 5. Conclusions

A single HIIT induces lactylation in tissues with high lactate uptake and metabolism, such as iWAT, BAT, soleus muscle and liver proteins, and K<sub>la</sub> levels peak at 24 h after HIIT and return to steady state levels at 72 h. However, the regulatory mechanisms need to be explored in depth. Lactylation proteins in iWAT may affect pathways related to glycolipid metabolism and are highly associated with de novo synthesis and energy metabolism. It is speculated that the changes in energy expenditure, lipolytic effects and metabolic characteristics during the recovery period after HIIT may be related to the regulation of protein lactylation in inguinal white adipose tissue.

**Author Contributions:** Conceptualization, J.Z.; methodology, J.Z.; software, W.H.; validation, W.H., J.S., S.L. and X.C.; formal analysis, W.H. and X.C.; resources, Y.L., Z.X. and L.G.; data curation, W.H.; writing—original draft preparation, W.H.; writing—review and editing, J.Z.; supervision, J.Z.; project administration, J.Z.; funding acquisition, J.Z. All authors have read and agreed to the published version of the manuscript.

**Funding:** This research was funded by the National Natural Science Foundation of China, grant number 31871207.

**Institutional Review Board Statement:** The study was approved by the guidelines of the Ethics and Animal Welfare Committee of Beijing Normal University (protocol code No. CLS-EAW-2015-002).

**Informed Consent Statement:** Not applicable.

**Data Availability Statement:** The original data of this study are available from the corresponding author upon reasonable request. The data are not publicly available due to being involved in another unpublished study.

**Conflicts of Interest:** The authors declare no conflict of interest.

## References

1. Zhang, D.; Tang, Z.; Huang, H.; Zhou, G.; Cui, C.; Weng, Y.; Liu, W.; Kim, S.; Lee, S.; Perez-Neut, M.; et al. Metabolic regulation of gene expression by histone lactylation. *Nature* **2019**, *574*, 575–580. [[CrossRef](#)] [[PubMed](#)]
2. Xiong, J.; He, J.; Zhu, J.; Pan, J.; Liao, W.; Ye, H.; Wang, H.; Song, Y.; Du, Y.; Cui, B.; et al. Lactylation-driven METTL3-mediated RNA m(6)A modification promotes immunosuppression of tumor-infiltrating myeloid cells. *Mol. Cell* **2022**, *82*, 1660–1677. [[CrossRef](#)] [[PubMed](#)]
3. Yu, J.; Chai, P.; Xie, M.; Ge, S.; Ruan, J.; Fan, X.; Jia, R. Histone lactylation drives oncogenesis by facilitating m(6)A reader protein YTHDF2 expression in ocular melanoma. *Genome Biol.* **2021**, *22*, 85. [[CrossRef](#)] [[PubMed](#)]
4. Yang, K.; Fan, M.; Wang, X.; Xu, J.; Wang, Y.; Tu, F.; Gill, P.S.; Ha, T.; Liu, L.; Williams, D.L.; et al. Lactate promotes macrophage HMGB1 lactylation, acetylation, and exosomal release in polymicrobial sepsis. *Cell Death Differ.* **2022**, *29*, 133–146. [[CrossRef](#)]
5. Hagihara, H.; Shoji, H.; Otabi, H.; Toyoda, A.; Katoh, K.; Namihira, M.; Miyakawa, T. Protein lactylation induced by neural excitation. *Cell Rep.* **2021**, *37*, 109820. [[CrossRef](#)] [[PubMed](#)]
6. Pan, R.Y.; He, L.; Zhang, J.; Liu, X.; Liao, Y.; Gao, J.; Liao, Y.; Yan, Y.; Li, Q.; Zhou, X.; et al. Positive feedback regulation of microglial glucose metabolism by histone H4 lysine 12 lactylation in Alzheimer's disease. *Cell Metab.* **2022**, *34*, 634–648. [[CrossRef](#)]

7. Logan, G.R.; Harris, N.; Duncan, S.; Schofield, G. A review of adolescent high-intensity interval training. *Sport. Med.* **2014**, *44*, 1071–1085. [[CrossRef](#)]
8. Liu, Q.Q.; Xie, W.Q.; Luo, Y.X.; Li, Y.D.; Huang, W.H.; Wu, Y.X.; Li, Y.S. High Intensity Interval Training: A Potential Method for Treating Sarcopenia. *Clin. Interv. Aging* **2022**, *17*, 857–872. [[CrossRef](#)]
9. Ross, L.M.; Porter, R.R.; Durstine, J.L. High-intensity interval training (HIIT) for patients with chronic diseases. *J. Sport Health Sci.* **2016**, *5*, 139–144. [[CrossRef](#)]
10. Fredrickson, G.; Barrow, F.; Dietsche, K.; Parthiban, P.; Khan, S.; Robert, S.; Demirchian, M.; Rhoades, H.; Wang, H.; Adeyi, O.; et al. Exercise of high intensity ameliorates hepatic inflammation and the progression of NASH. *Mol. Metab.* **2021**, *53*, 101270. [[CrossRef](#)]
11. Lovatel, G.A.; Elsner, V.R.; Bertoldi, K.; Vanzella, C.; Moyses, F.S.; Vizuete, A.; Spindler, C.; Cechinel, L.R.; Netto, C.A.; Muotri, A.R.; et al. Treadmill exercise induces age-related changes in aversive memory, neuroinflammatory and epigenetic processes in the rat hippocampus. *Neurobiol. Learn. Mem.* **2013**, *101*, 94–102. [[CrossRef](#)] [[PubMed](#)]
12. Overmyer, K.A.; Evans, C.R.; Qi, N.R.; Minogue, C.E.; Carson, J.J.; Chermiside-Scabbo, C.J.; Koch, L.G.; Britton, S.L.; Pagliarini, D.J.; Coon, J.J.; et al. Maximal oxidative capacity during exercise is associated with skeletal muscle fuel selection and dynamic changes in mitochondrial protein acetylation. *Cell Metab.* **2015**, *21*, 468–478. [[CrossRef](#)] [[PubMed](#)]
13. Huang, W.H.; Zhang, J.B.; Chen, X.F.; Zhang, J. Research progress of exercise and protein acylation. *Prog. Biochem. Biophys.* **2022**, *49*, 454–467. [[CrossRef](#)]
14. Liang, F.; Huang, T.; Li, B.; Zhao, Y.; Zhang, X.; Xu, B. High-intensity interval training and moderate-intensity continuous training alleviate beta-amyloid deposition by inhibiting NLRP3 inflammasome activation in APP<sup>swe</sup>/PS1<sup>dE9</sup> mice. *Neuroreport* **2020**, *31*, 425–432. [[CrossRef](#)] [[PubMed](#)]
15. Brooks, G.A. The tortuous path of lactate shuttle discovery: From cinders and boards to the lab and ICU. *J. Sport Health Sci.* **2020**, *9*, 446–460. [[CrossRef](#)]
16. Fisel, P.; Schaeffeler, E.; Schwab, M. Clinical and Functional Relevance of the Monocarboxylate Transporter Family in Disease Pathophysiology and Drug Therapy. *Clin. Transl. Sci.* **2018**, *11*, 352–364. [[CrossRef](#)]
17. Adeva-Andany, M.; Lopez-Ojen, M.; Funcasta-Calderon, R.; Ameneiros-Rodriguez, E.; Donapetry-Garcia, C.; Vila-Altesor, M.; Rodriguez-Seijas, J. Comprehensive review on lactate metabolism in human health. *Mitochondrion* **2014**, *17*, 76–100. [[CrossRef](#)]
18. Mu, W.J.; Zhu, J.Y.; Chen, M.; Guo, L. Exercise-Mediated Browning of White Adipose Tissue: Its Significance, Mechanism and Effectiveness. *Int. J. Mol. Sci.* **2021**, *22*, 11512. [[CrossRef](#)]
19. Carriere, A.; Lagarde, D.; Jeanson, Y.; Portais, J.C.; Galinier, A.; Ader, I.; Casteilla, L. The emerging roles of lactate as a redox substrate and signaling molecule in adipose tissues. *J. Physiol. Biochem.* **2020**, *76*, 241–250. [[CrossRef](#)]
20. Joseph, J.S.; Ayeleso, A.O.; Mukwevho, E. Exercise increases hyper-acetylation of histones on the Cis-element of NRF-1 binding to the Mef2a promoter: Implications on type 2 diabetes. *Biochem. Biophys. Res. Commun.* **2017**, *486*, 83–87. [[CrossRef](#)]
21. Masuzawa, R.; Konno, R.; Ohsawa, I.; Watanabe, A.; Kawano, F. Muscle type-specific RNA polymerase II recruitment during PGC-1 $\alpha$  gene transcription after acute exercise in adult rats. *J. Appl. Physiol.* **2018**, *125*, 1238–1245. [[CrossRef](#)] [[PubMed](#)]
22. Seaborne, R.A.; Sharples, A.P. The Interplay Between Exercise Metabolism, Epigenetics, and Skeletal Muscle Remodeling. *Exerc. Sport Sci. Rev.* **2020**, *48*, 188–200. [[CrossRef](#)] [[PubMed](#)]
23. Evans, M.; Cogan, K.E.; Egan, B. Metabolism of ketone bodies during exercise and training: Physiological basis for exogenous supplementation. *J. Physiol.* **2017**, *595*, 2857–2871. [[CrossRef](#)] [[PubMed](#)]
24. Nasser, S.; Sole, T.; Vega, N.; Thomas, T.; Balcerzyk, A.; Strigini, M.; Pirola, L. Ketogenic diet administration to mice after a high-fat-diet regimen promotes weight loss, glycemic normalization and induces adaptations of ketogenic pathways in liver and kidney. *Mol. Metab.* **2022**, *65*, 101578. [[CrossRef](#)]
25. Yao, Y.; Bade, R.; Li, G.; Zhang, A.; Zhao, H.; Fan, L.; Zhu, R.; Yuan, J. Global-Scale Profiling of Differential Expressed Lysine-Lactylated Proteins in the Cerebral Endothelium of Cerebral Ischemia-Reperfusion Injury Rats. *Cell. Mol. Neurobiol.* **2022**. [[CrossRef](#)]
26. Enoki, T.; Yoshida, Y.; Lally, J.; Hatta, H.; Bonen, A. Testosterone increases lactate transport, monocarboxylate transporter (MCT) 1 and MCT4 in rat skeletal muscle. *J. Physiol.* **2006**, *577*, 433–443. [[CrossRef](#)]
27. Latham, T.; Mackay, L.; Sproul, D.; Karim, M.; Culley, J.; Harrison, D.J.; Hayward, L.; Langridge-Smith, P.; Gilbert, N.; Ramsahoye, B.H. Lactate, a product of glycolytic metabolism, inhibits histone deacetylase activity and promotes changes in gene expression. *Nucleic Acids Res.* **2012**, *40*, 4794–4803. [[CrossRef](#)]
28. Feng, Q.; Liu, Z.; Yu, X.; Huang, T.; Chen, J.; Wang, J.; Wilhelm, J.; Li, S.; Song, J.; Li, W.; et al. Lactate increases stemness of CD8 + T cells to augment anti-tumor immunity. *Nat. Commun.* **2022**, *13*, 4981. [[CrossRef](#)]
29. Moreno-Yruela, C.; Zhang, D.; Wei, W.; Baek, M.; Liu, W.; Gao, J.; Dankova, D.; Nielsen, A.L.; Bolding, J.E.; Yang, L.; et al. Class I histone deacetylases (HDAC1-3) are histone lysine delactylases. *Sci. Adv.* **2022**, *8*, i6696. [[CrossRef](#)]
30. Diniz, T.A.; Aquino, J.J.; Mosele, F.C.; Cabral-Santos, C.; Lima, J.E.; Teixeira, A.; Lira, F.S.; Rosa, N.J. Exercise-induced AMPK activation and IL-6 muscle production are disturbed in adiponectin knockout mice. *Cytokine* **2019**, *119*, 71–80. [[CrossRef](#)]
31. Parker, B.L.; Kiens, B.; Wojtaszewski, J.; Richter, E.A.; James, D.E. Quantification of exercise-regulated ubiquitin signaling in human skeletal muscle identifies protein modification cross talk via NEDDylation. *FASEB J.* **2020**, *34*, 5906–5916. [[CrossRef](#)] [[PubMed](#)]

32. Peternelj, T.T.; Marsh, S.A.; Strobel, N.A.; Matsumoto, A.; Briskey, D.; Dalbo, V.J.; Tucker, P.S.; Coombes, J.S. Glutathione depletion and acute exercise increase O-GlcNAc protein modification in rat skeletal muscle. *Mol. Cell. Biochem.* **2015**, *400*, 265–275. [[CrossRef](#)] [[PubMed](#)]
33. Cui, H.; Xie, N.; Banerjee, S.; Ge, J.; Jiang, D.; Dey, T.; Matthews, Q.L.; Liu, R.M.; Liu, G. Lung Myofibroblasts Promote Macrophage Profibrotic Activity through Lactate-induced Histone Lactylation. *Am. J. Respir. Cell Mol. Biol.* **2021**, *64*, 115–125. [[CrossRef](#)]
34. Uekawa, A.; Yamanaka, H.; Lieben, L.; Kimira, Y.; Uehara, M.; Yamamoto, Y.; Kato, S.; Ito, K.; Carmeliet, G.; Masuyama, R. Phosphate-dependent luminal ATP metabolism regulates transcellular calcium transport in intestinal epithelial cells. *FASEB J.* **2018**, *32*, 1903–1915. [[CrossRef](#)]
35. Hopp, A.K.; Gruter, P.; Hottiger, M.O. Regulation of Glucose Metabolism by NAD(+) and ADP-Ribosylation. *Cells* **2019**, *8*, 890. [[CrossRef](#)]
36. Covarrubias, A.J.; Perrone, R.; Grozio, A.; Verdin, E. NAD(+) metabolism and its roles in cellular processes during ageing. *Nat. Rev. Mol. Cell Biol.* **2021**, *22*, 119–141. [[CrossRef](#)]
37. Peng, H.; Wang, Y.; Luo, W. Multifaceted role of branched-chain amino acid metabolism in cancer. *Oncogene* **2020**, *39*, 6747–6756. [[CrossRef](#)]
38. Yuan, Y.; Xu, P.; Jiang, Q.; Cai, X.; Wang, T.; Peng, W.; Sun, J.; Zhu, C.; Zhang, C.; Yue, D.; et al. Exercise-induced alpha-ketoglutaric acid stimulates muscle hypertrophy and fat loss through OXGR1-dependent adrenal activation. *EMBO J.* **2021**, *40*, e108434. [[CrossRef](#)] [[PubMed](#)]
39. Acin-Perez, R.; Petcherski, A.; Veliova, M.; Benador, I.Y.; Assali, E.A.; Colleluori, G.; Cinti, S.; Brownstein, A.J.; Baghdasarian, S.; Livhits, M.J.; et al. Recruitment and remodeling of peridroplet mitochondria in human adipose tissue. *Redox Biol.* **2021**, *46*, 102087. [[CrossRef](#)]
40. Brooks, G.A. Lactate as a fulcrum of metabolism. *Redox Biol.* **2020**, *35*, 101454. [[CrossRef](#)]
41. Colak, E.; Pap, D. The role of oxidative stress in the development of obesity and obesity-related metabolic disorders. *J. Med. Biochem.* **2021**, *40*, 1–9. [[CrossRef](#)] [[PubMed](#)]
42. Sindorf, M.; Germano, M.D.; Dias, W.G.; Batista, D.R.; Braz, T.V.; Moreno, M.A.; Lopes, C.R. Excess Post-Exercise Oxygen Consumption and Substrate Oxidation Following High-Intensity Interval Training: Effects of Recovery Manipulation. *Int. J. Exerc. Sci.* **2021**, *14*, 1151–1165. [[PubMed](#)]
43. Gu, L.; Zhu, Y.; Lin, X.; Lu, B.; Zhou, X.; Zhou, F.; Zhao, Q.; Prochownik, E.V.; Li, Y. The IKKbeta-USP30-ACLY Axis Controls Lipogenesis and Tumorigenesis. *Hepatology* **2021**, *73*, 160–174. [[CrossRef](#)] [[PubMed](#)]
44. Batchuluun, B.; Pinkosky, S.L.; Steinberg, G.R. Lipogenesis inhibitors: Therapeutic opportunities and challenges. *Nat. Rev. Drug Discov.* **2022**, *21*, 283–305. [[CrossRef](#)]
45. Lin, H.P.; Cheng, Z.L.; He, R.Y.; Song, L.; Tian, M.X.; Zhou, L.S.; Groh, B.S.; Liu, W.R.; Ji, M.B.; Ding, C.; et al. Destabilization of Fatty Acid Synthase by Acetylation Inhibits De Novo Lipogenesis and Tumor Cell Growth. *Cancer Res.* **2016**, *76*, 6924–6936. [[CrossRef](#)]
46. Lin, R.; Tao, R.; Gao, X.; Li, T.; Zhou, X.; Guan, K.L.; Xiong, Y.; Lei, Q.Y. Acetylation stabilizes ATP-citrate lyase to promote lipid biosynthesis and tumor growth. *Mol. Cell.* **2013**, *51*, 506–518. [[CrossRef](#)]
47. Xu, H.; Wu, M.; Ma, X.; Huang, W.; Xu, Y. Function and Mechanism of Novel Histone Posttranslational Modifications in Health and Disease. *Biomed. Res. Int.* **2021**, *2021*, 6635225. [[CrossRef](#)]
48. Gao, R.; Li, Y.; Xu, Z.; Zhang, F.; Xu, J.; Hu, Y.; Yin, J.; Yang, K.; Sun, L.; Wang, Q.; et al. Mitochondrial pyruvate carrier 1 regulates fatty acid synthase lactylation and mediates treatment of nonalcoholic fatty liver disease. *Hepatology* **2023**. [[CrossRef](#)]

**Disclaimer/Publisher’s Note:** The statements, opinions and data contained in all publications are solely those of the individual author(s) and contributor(s) and not of MDPI and/or the editor(s). MDPI and/or the editor(s) disclaim responsibility for any injury to people or property resulting from any ideas, methods, instructions or products referred to in the content.